

Electronic Supplemental Information

for

**Visible Light Induced Formation of a Tungsten
Hydride Complex**

Diane P. Isaacs, Cole T. Gruninger, Tao Huang, Aldo M. Jordan, Genique Nicholas, Chun-
Hsing Chen, Marc A. ter Horst, Jillian L. Dempsey*

*Department of Chemistry, University of North Carolina at Chapel Hill, Chapel Hill, North Carolina
27599-3290, United States*

**Correspondence to: dempseyj@email.unc.edu*

Table of Contents

I.	Control Experiments	S2
II.	Computational Details and Methods	S10
III.	Sample Computational Input Files	S10
IV.	Coordinates for Optimized Geometry of $[\text{CpW}(\text{CO})_3]_2$ Used in TD-DFT Calculations	S14
V.	Crystallographic Details for $[\text{CpW}(\text{CO})_3(\text{NCCH}_3)][\text{PF}_6]$	S15
VI.	Actinometry Experiments Using Potassium Ferrioxalate	S19
	Calibration Curve	S20
VII.	Steady-state Approximation	S22
VIII.	References	S24

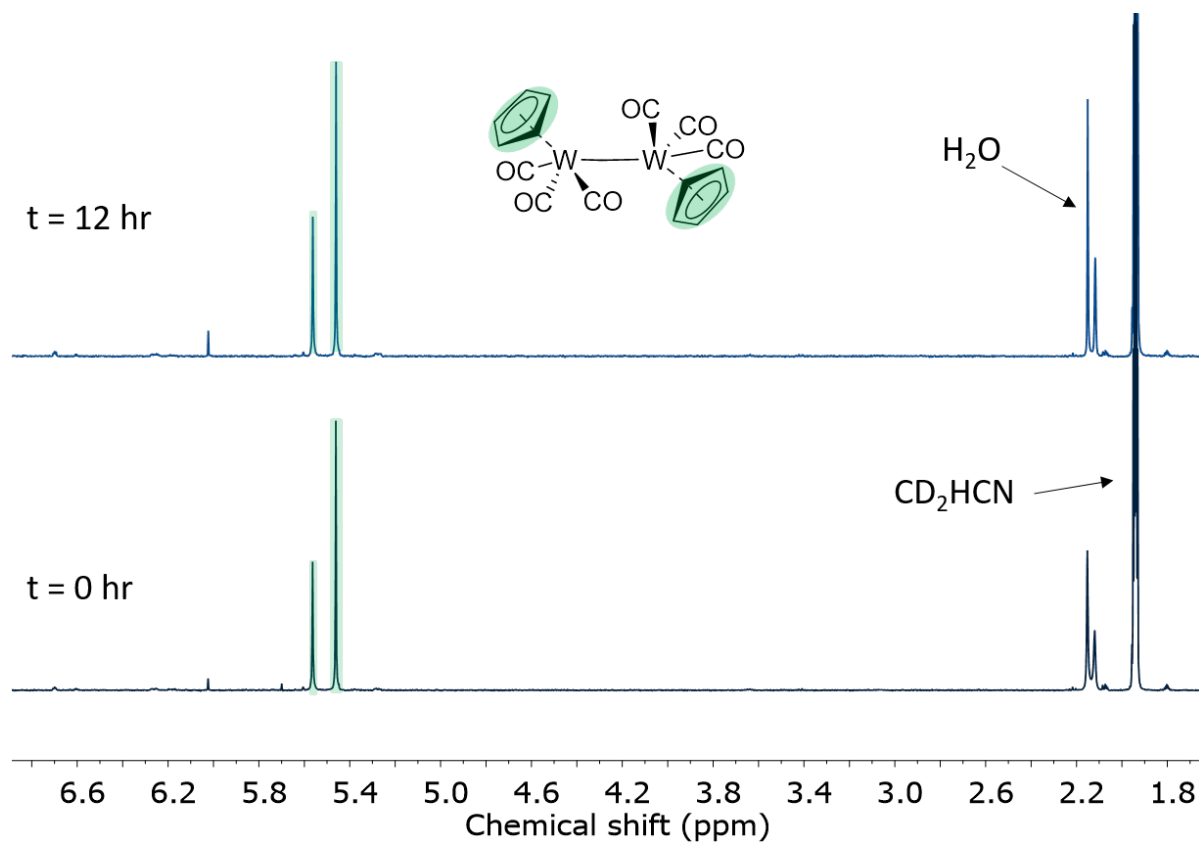


Figure S1. ¹H NMR spectra before and after heating [CpW(CO)₃]₂ at 80° C for a period of 12 consecutive hours. The cis (δ 5.59) and trans (δ 5.49) Cp peaks of the [CpW(CO)₃]₂ dimer are highlighted in green for clarity. Integration of both peaks with reference to an internal standard (1, 3, 5- trimethoxybenzene) before and after heating indicates a <10% change in the overall area and minimal degradation or thermal disproportionation had taken place.

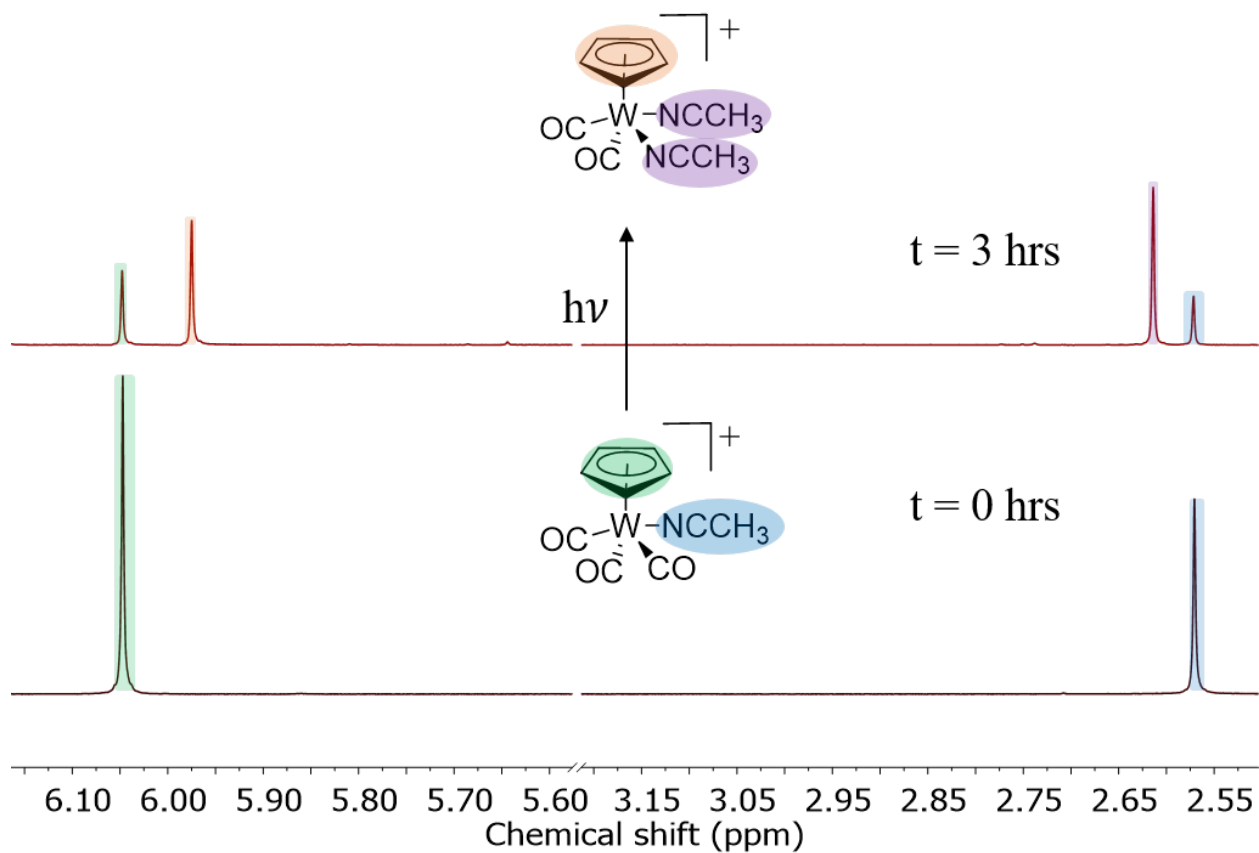


Figure S2. (Bottom) ^1H NMR spectra of the synthetically isolated $[\text{CpW}(\text{CO})_3(\text{NCCH}_3)]^+[\text{PF}_6]^-$ before performing bulk photolysis in acetonitrile. (Top) ^1H NMR spectrum of the same species after photolysis for 3 consecutive hours at 450 nm in proteo- acetonitrile solvent. After photolysis, the resultant solution was dried down under vacuum and re-dissolved in CD_3CN to take an ^1H NMR spectrum. Two new peaks (δ 6.01 and δ 2.61) were observed in the product, in addition to the starting material, with an integration ratio of 5:6 indicating the formation of the CO-loss product $[\text{CpW}(\text{CO})_2(\text{NCCH}_3)_2]^+$. The Cp and bound acetonitrile peaks of $[\text{CpW}(\text{CO})_3(\text{NCCH}_3)]^+$ and $[\text{CpW}(\text{CO})_2(\text{NCCH}_3)_2]^+$ are highlighted above for clarity.

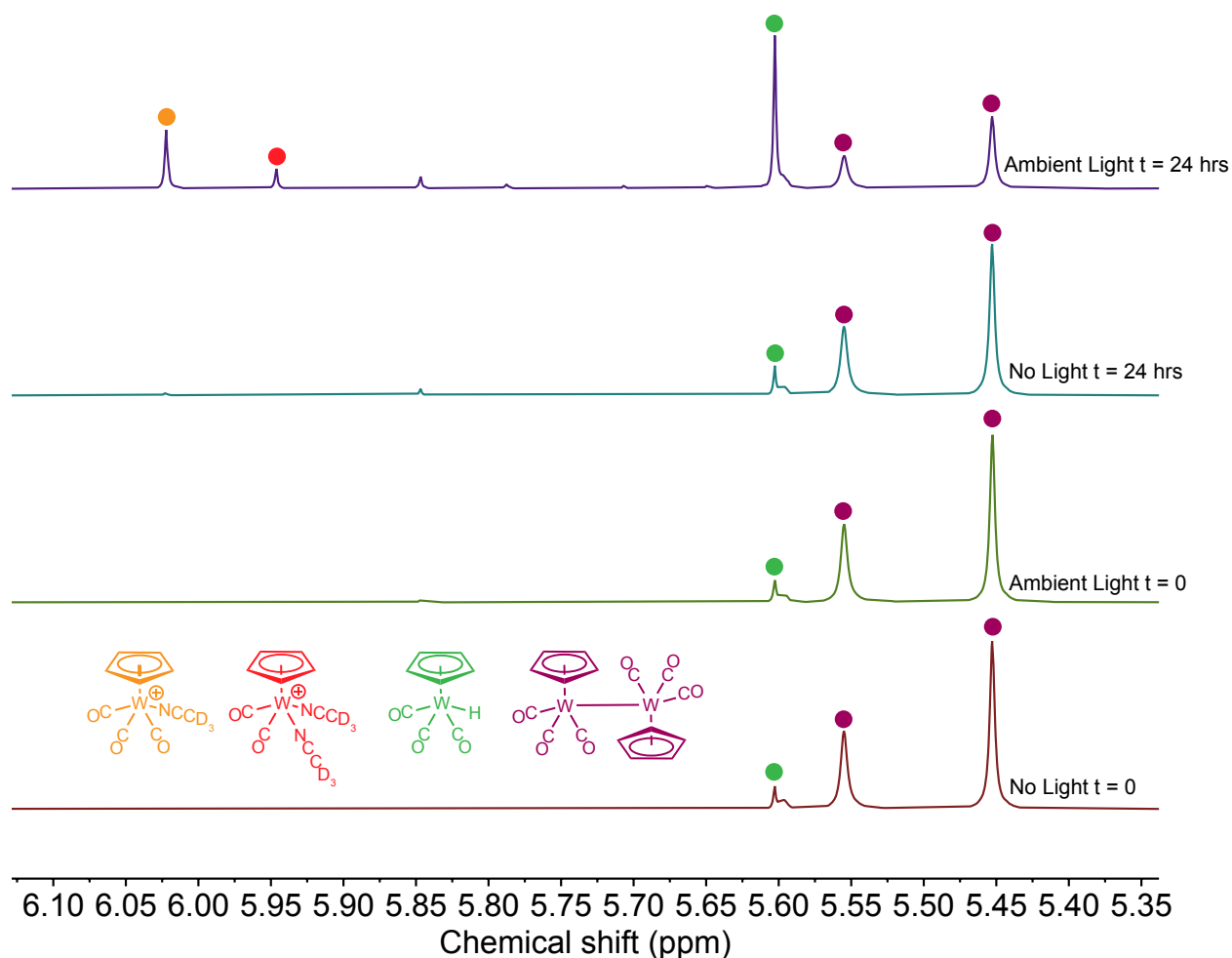


Figure S3. (Bottom–top) Initial ^1H NMR spectra of tube 1 of $[\text{CpW}(\text{CO})_3]_2$ and $[\text{PyH}][\text{BF}_4]$ shielded from ambient light with aluminum foil, initial ^1H NMR spectra of tube 2 of $[\text{CpW}(\text{CO})_3]_2$ and $[\text{PyH}][\text{BF}_4]$ before exposed to ambient light, ^1H NMR spectra of tube 1 of $[\text{CpW}(\text{CO})_3]_2$ and $[\text{PyH}][\text{BF}_4]$ shielded from ambient light with aluminum foil for 24 hrs, and ^1H NMR spectra of tube 2 of $[\text{CpW}(\text{CO})_3]_2$ and $[\text{PyH}][\text{BF}_4]$ after being exposed to ambient light for 24 hrs. Delay time for all ^1H NMR spectra was 60s. Table S1 has the concentrations of $[\text{CpW}(\text{CO})_3]_2$ and $\text{CpW}(\text{CO})_3\text{H}$ for all spectra.

Table S1 Concentrations of $[\text{CpW}(\text{CO})_3]_2$ and $\text{CpW}(\text{CO})_3\text{H}$ calculated from the internal standard, biphenyl, for all spectra in the ambient light control.

Sample	Concentration of $\text{CpW}(\text{CO})_3\text{H}$ (mM)	Concentration of $[\text{CpW}(\text{CO})_3]_2$ (mM)
No Light t = 0	0.13	3.2
Ambient Light t = 0	0.13	3.2
No Light t = 24 hrs	0.16	3.0
Ambient Light t = 24 hrs	0.83	1.5

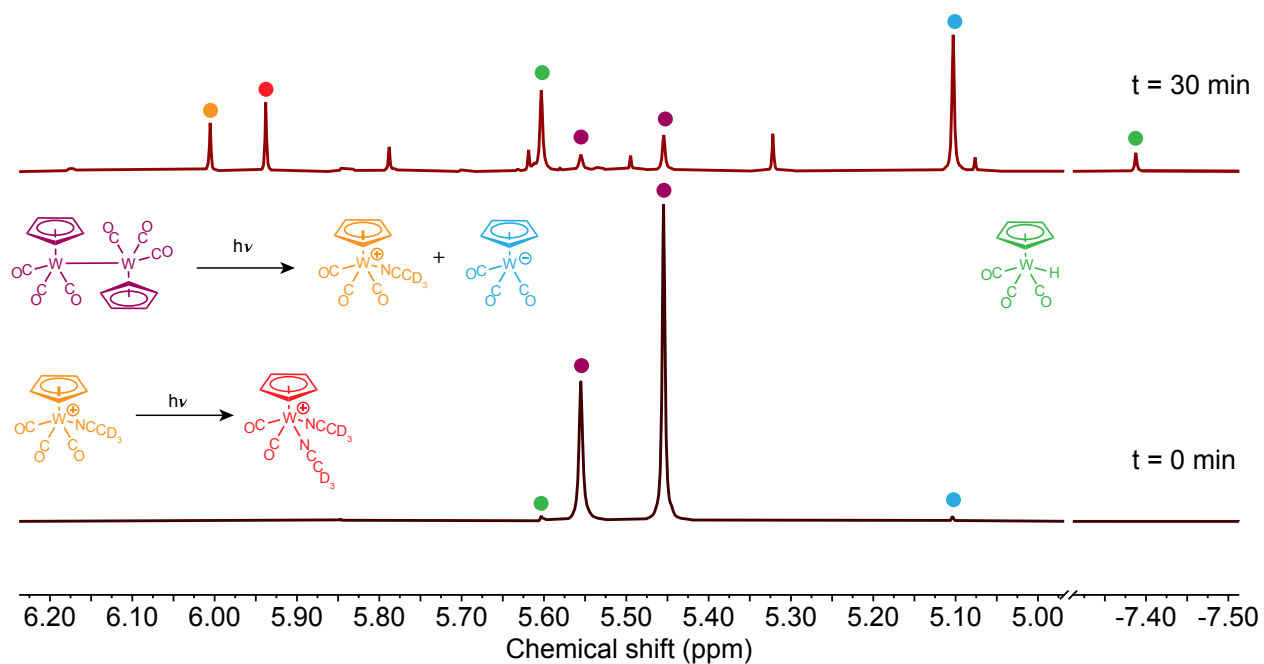


Figure S4. (Bottom) ^1H NMR spectra of the $[\text{CpW}(\text{CO})_3]_2$ dimer (2.03 mM) in a solution of CD_3CN before photolysis. No $[\text{PyH}][\text{BF}_4]$ is present in this sample. (Top) ^1H NMR spectrum of the same solution after 30 min of photolysis at 455 nm. Delay time for ^1H NMR was 60s.

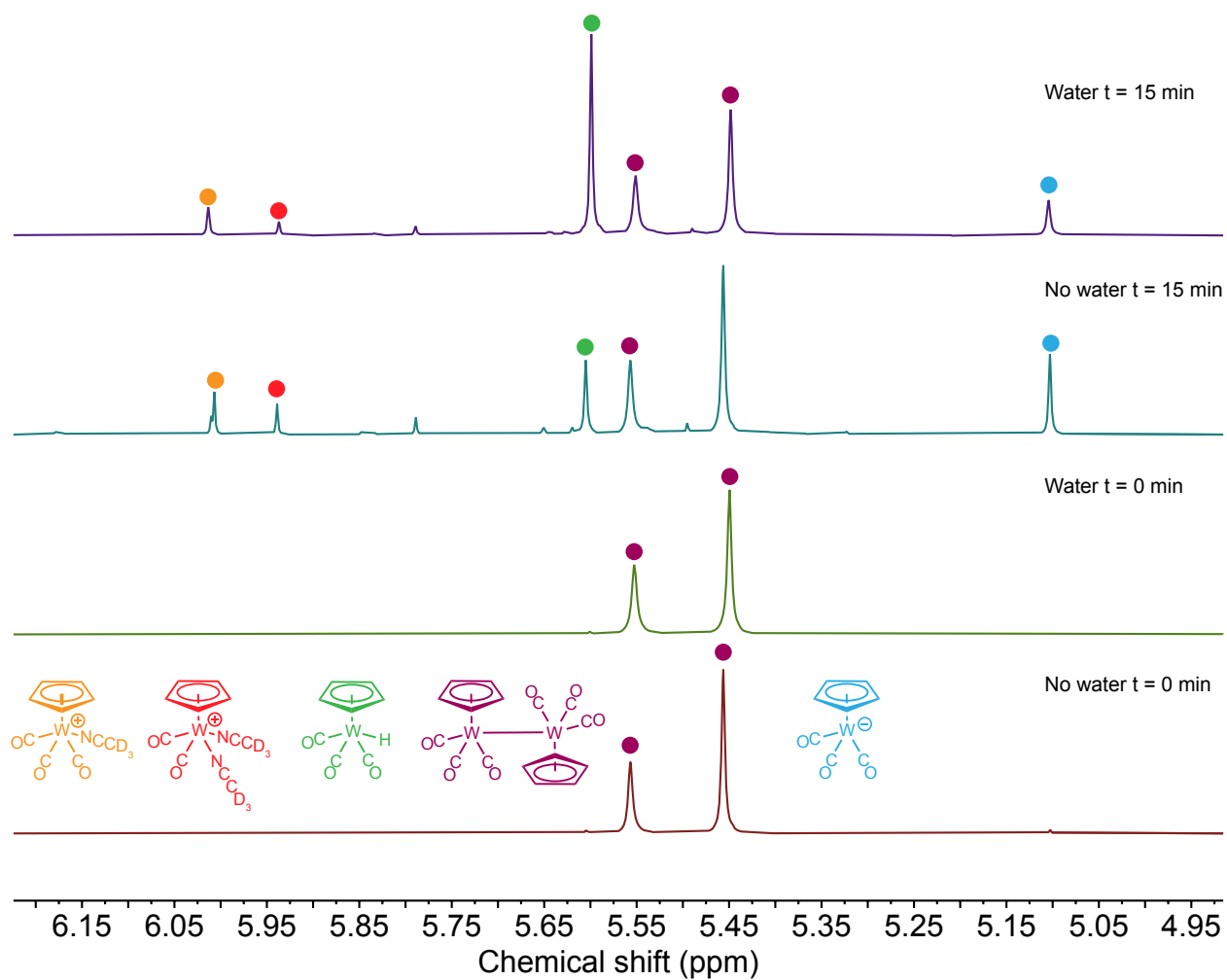


Figure S5 (Bottom–top) Initial ^1H NMR spectra of tube 1 of $[\text{CpW}(\text{CO})_3]_2$, initial ^1H NMR spectra of tube 2 of $[\text{CpW}(\text{CO})_3]_2$ and 1.1 mM water, ^1H NMR spectra of tube 1 of $[\text{CpW}(\text{CO})_3]_2$ after 15 min irradiation with 455nm light, and ^1H NMR spectra of tube 2 of $[\text{CpW}(\text{CO})_3]_2$ and water after 15 min irradiation with 455nm light. Delay time for all ^1H NMR spectra was 60s.

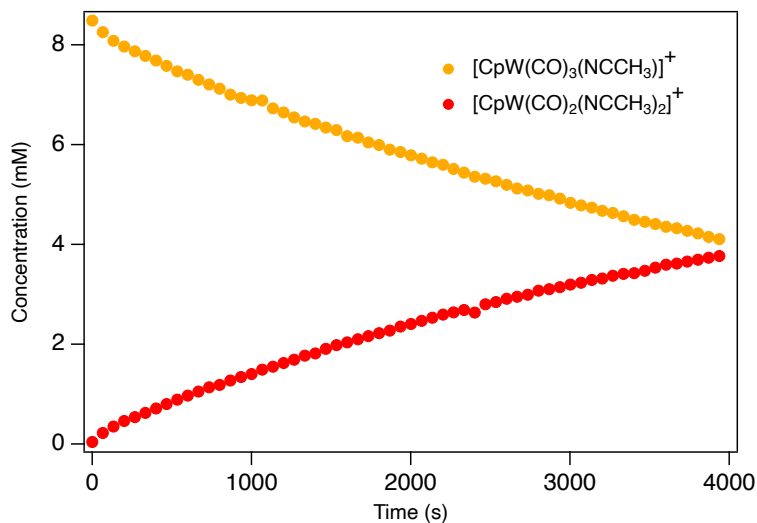


Figure S6. Concentrations $[\text{CpW}(\text{CO})_3(\text{NCCH}_3)]^+$ (orange) and $[\text{CpW}(\text{CO})_2(\text{NCCH}_3)_2]^+$ (red) upon continuous photolysis of $[\text{CpW}(\text{CO})_3(\text{NCCH}_3)]^+$ in CD_3CN at various time delays. Individual time points were recorded *in situ* using the Prizmatix 450nm LED lamp at an intensity setting of 3. The experiment was collected as 60 single scan spectra with 60 s delay time and a 0 s fixed delay between scans. Concentrations were computed by integration of the 6.05 ppm peak for $[\text{CpW}(\text{CO})_3(\text{NCCH}_3)]^+$ and 6.01 ppm peak for $[\text{CpW}(\text{CO})_2(\text{NCCH}_3)_2]^+$ in individual ^1H NMR spectra at each time delay with reference to biphenyl as an internal standard.

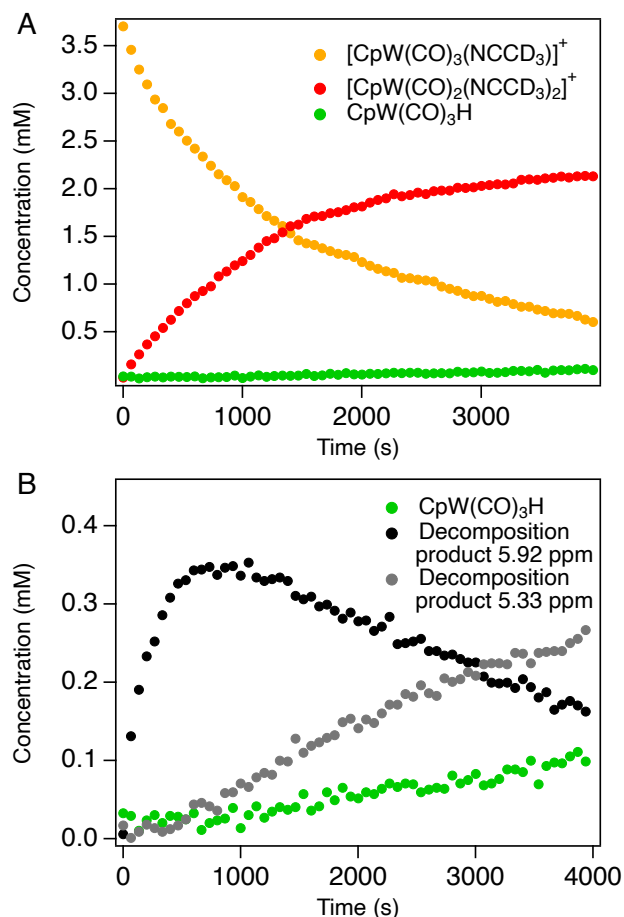


Figure S7. (A) Concentrations of $[\text{CpW}(\text{CO})_3(\text{NCCH}_3)]^+$ (orange), $[\text{CpW}(\text{CO})_2(\text{NCCH}_3)_2]^+$ (red), and $\text{CpW}(\text{CO})_3\text{H}$ (green) at various time delays for the continuous photolysis reaction of $[\text{CpW}(\text{CO})_3(\text{NCCH}_3)]^+$ in the presence of 70.1 mM $[\text{PyH}][\text{BF}_4]$. Concentrations are computed by integration of the 6.05 ppm peak for $[\text{CpW}(\text{CO})_3(\text{NCCH}_3)]^+$, 6.01 ppm peak for $[\text{CpW}(\text{CO})_2(\text{NCCH}_3)_2]^+$, and 5.63 ppm for $\text{CpW}(\text{CO})_3\text{H}$ in the individual ^1H NMR spectra at each time delay with reference to biphenyl as an internal standard. Individual time points were recorded *in situ* using the Prizmatix 450nm LED lamp at an intensity setting of 3. The experiment was collected as 60 single scan spectra with 60 s delay time and a 0 s fixed delay between scans. (B) Concentrations of $\text{CpW}(\text{CO})_3\text{H}$ (green), and unidentified decomposition products (black and gray) for the same reaction in panel A as a function of time.

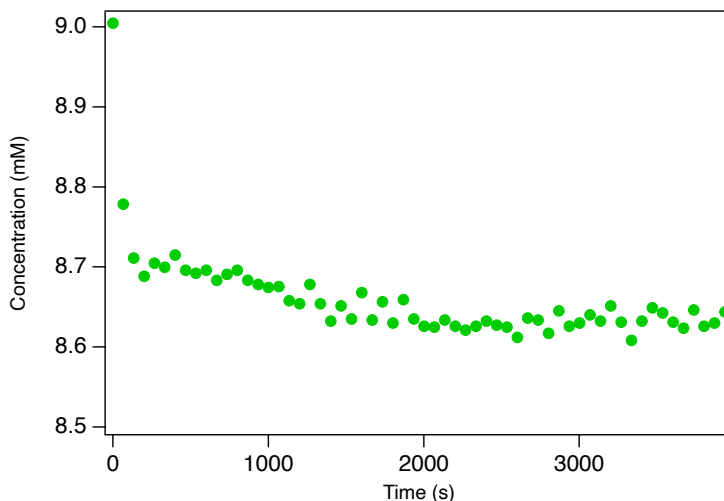


Figure S8. Concentration of $\text{CpW}(\text{CO})_3\text{H}$ in CD_3CN under continuous photolysis conditions. Individual time points were recorded *in situ* using the Prizmatix 450nm LED lamp at an intensity setting of 3. The experiment was collected as 60 single scan spectra with 60 s delay time and a 0 s fixed delay between scans. Concentrations are computed by integration of the 5.63 ppm peak in the individual ^1H NMR spectra at each time delay with reference to trimethoxy benzene as an internal standard.

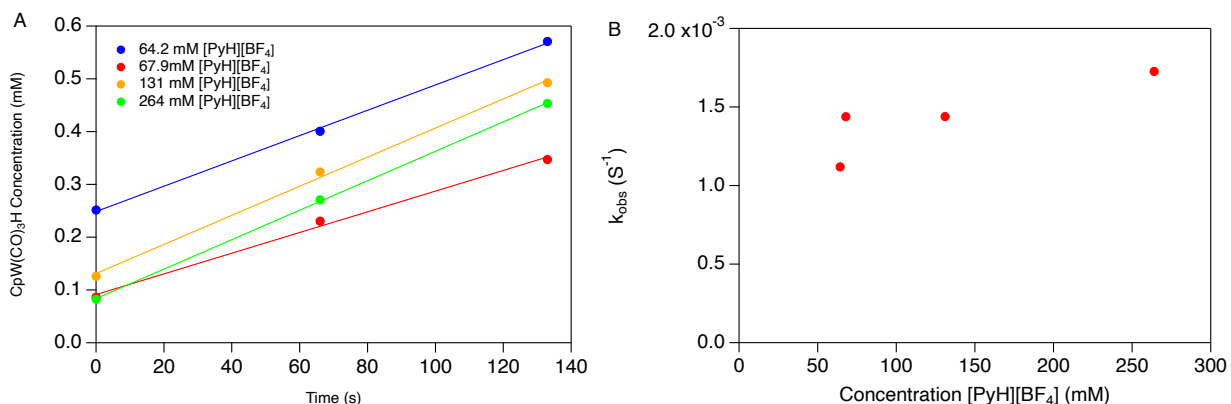


Figure S9. (A) Concentration of $\text{CpW}(\text{CO})_3\text{H}$ product vs. time for the photolysis of $[\text{CpW}(\text{CO})_3]_2$ at 450 nm in the presence $[\text{PyH}][\text{BF}_4]$ at four different concentrations. Linear regression of concentration–time traces are as follows: (64.2mM) $y = 0.0024x + 0.2486$; (67.9 mM) $y = 0.0020x + 0.0914$; (131 mM) $y = 0.0028x + 0.1313$; (264 mM) $y = 0.0028x + 0.0838$. (B) Rate constants k_{obs} , obtained from linear regression in panel A, are plotted versus the $[\text{PyH}][\text{BF}_4]$ concentration used.

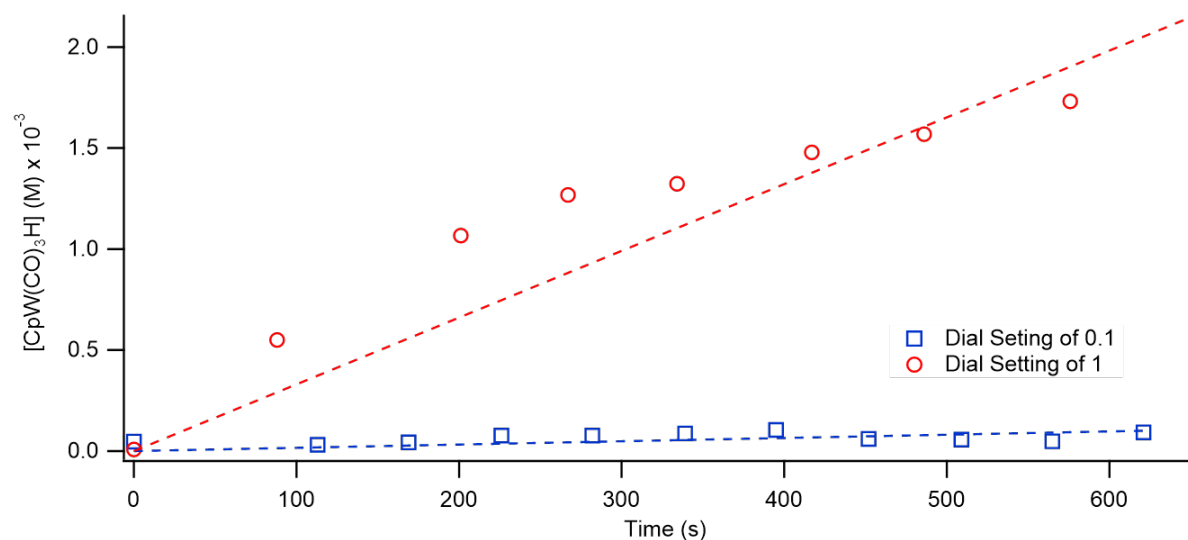


Figure S10. Concentration vs. time profiles monitoring the formation of $\text{CpW}(\text{CO})_3\text{H}$ upon photolysis of $[\text{CpW}(\text{CO})_3]_2$ at 450 nm in the presence of 10 eq. of $[\text{PyH}][\text{BF}_4]$ at two different light intensities. Data recorded *in situ*, with lamp intensity modulated by the analog dial. Linear fits are included to highlight the disparity between rates of formation at the two different dial settings.

Computational Details and Methods

Geometry optimizations. The geometry of $[\text{CpW}(\text{CO})_3]_2$ was optimized using the B3LYP functional and LANL2DZ basis set for W and 6-31G* for all other atoms. A sample input file for the geometry optimization is shown in section III below and the optimized coordinates for all complexes using B3LYP are listed in section IV.

Electronic structure calculations. The first 12 excitations of were calculated for $[\text{CpW}(\text{CO})_3]_2$ using the B3LYP functional. Calculations were analyzed using the Chemcraftsuite with orbitals depicted with a contour value of 0.045. A sample input file for the TD-DFT calculation shown in section III.

Sample Input Files for Calculations

- Sample input file for geometry optimization and frequency analysis

```
%chk=[CpW(CO)3]2_Optimization.chk

%mem=1600MB

%nprocshared=8

# opt freq b3lyp/genecp pop=full geom=connectivity scf=(conver=8,maxcycle=200)
```

[CpW(CO)3]2_Optimization

0 1

C	0	1.14900000	1.70600000	0.52400000	L
C	0	1.34300000	-2.34300000	1.60700000	L
C	0	1.97800000	-1.94000000	0.41900000	L
C	0	2.96600000	-0.94500000	0.75200000	L
C	0	2.92200000	-0.79100000	2.16000000	L
C	0	1.91700000	-1.64800000	2.65800000	L
C	0	0.80600000	1.14000000	2.90100000	L
C	0	-1.07700000	-0.16100000	1.81000000	L
H	0	0.74800000	-2.94100000	1.68000000	L
H	0	1.75000000	-2.41500000	-0.52700000	L
H	0	3.59500000	-0.31100000	0.10700000	L
H	0	3.39100000	-0.19100000	2.55900000	L
H	0	1.74400000	-1.69000000	3.38900000	L
O	0	1.39800000	2.75600000	0.11300000	L
O	0	0.80300000	1.83900000	3.83100000	L
O	0	-2.13900000	-0.27500000	2.18200000	L
W	0	0.86400000	-0.06200000	1.35900000	L
W	0	-0.86400000	0.06200000	-1.35900000	L
C	0	-1.14900000	-1.70600000	-0.52400000	L
C	0	-1.34300000	2.34300000	-1.60700000	L
C	0	-1.97800000	1.94000000	-0.41900000	L
C	0	-2.96600000	0.94500000	-0.75200000	L
C	0	-2.92200000	0.79100000	-2.16000000	L
C	0	-1.91700000	1.64800000	-2.65800000	L
C	0	-0.80600000	-1.14000000	-2.90100000	L
C	0	1.07700000	0.16100000	-1.81000000	L
O	0	-1.39800000	-2.75600000	-0.11300000	L
H	0	-0.74800000	2.94100000	-1.68000000	L
H	0	-1.75000000	2.41500000	0.52700000	L
H	0	-3.59500000	0.31100000	-0.10700000	L
H	0	-3.39100000	0.19100000	-2.55900000	L
H	0	-1.74400000	1.69000000	-3.38900000	L
O	0	-0.80300000	-1.83900000	-3.83100000	L
O	0	2.13900000	0.27500000	-2.18200000	L

1 17 1.0 14 3.0
2 3 1.5 6 2.0 9 1.0
3 4 1.5 10 1.0
4 5 1.5 11 1.0
5 6 1.5 12 1.0
6 13 1.0
7 17 1.0 15 2.0
8 16 3.0 17 1.0
9
10
11
12
13
14
15
16

```
17 18 1.0
18 25 1.0 19 1.0 26 1.0
19 27 3.0
20 24 2.0 28 1.0 21 1.5
21 22 1.5 29 1.0
22 23 1.5 30 1.0
23 24 1.5 31 1.0
24 32 1.0
25 33 2.0
26 34 3.0
27
28
29
30
31
32
33
34
```

```
C H O O
6-31g(d',p')
****
```

```
W 0
LANL2DZ
****
```

```
W 0
LANL2DZ
```

b. Sample input file for computing the first 12 vertical excited states transitions

```
%chk=CpWCO32_TD_DFT.chk
```

```
%mem=1600MB
```

```
%nprocshared=8
```

```
# td=(nstates=12) b3lyp/genecp pop=full density=current geom=connectivity
```

```
scf=(conver=8,maxcycle=200)
```

```
CpWCO32_TD_DFT
```

```
0 1
C          0.96788879   1.06864502  -1.58541684
C          2.31778813  -1.90840599   1.15738207
```

C	1.60497479	-2.33819046	-0.00082494
C	2.31880913	-1.90780341	-1.15819751
C	3.48504084	-1.21583361	-0.71894715
C	3.48444858	-1.21622841	0.71946034
C	2.85928072	1.67565331	0.00022141
C	0.96805612	1.06801307	1.58590852
H	2.02294345	-2.08809703	2.18302178
H	0.68148407	-2.90084307	-0.00153240
H	2.02441333	-2.08659844	-2.18414067
H	4.25359630	-0.79506903	-1.35507228
H	4.25255343	-0.79611373	1.35660029
O	0.65249319	1.62395977	-2.55566960
O	3.58767721	2.57580986	0.00024553
O	0.65249383	1.62292352	2.55635490
W	1.66558475	0.09420967	0.00002236
W	-1.66554072	-0.09416419	-0.00003800
C	-0.96793985	-1.06865483	1.58540393
C	-2.31788549	1.90844219	-1.15739537
C	-1.60514708	2.33825725	0.00084499
C	-2.31897944	1.90778061	1.15818556
C	-3.48513860	1.21572526	0.71887714
C	-3.48449912	1.21615198	-0.71952519
C	-2.85916935	-1.67564570	-0.00028602
C	-0.96798986	-1.06803554	-1.58583311
O	-0.65266524	-1.62405568	2.55564344
H	-2.02301478	2.08817328	-2.18302392
H	-0.68168753	2.90096478	0.00159309
H	-2.02462745	2.08657224	2.18413988
H	-4.25366602	0.79485454	1.35496661
H	-4.25254352	0.79597428	-1.35669634
O	-3.58731625	-2.57600389	0.00005314
O	-0.65267519	-1.62293446	-2.55635811

1 14 3.0 17 1.0

2 3 1.5 6 2.0 9 1.0 17 0.1

3 4 1.5 10 1.0 17 0.1

4 5 1.5 11 1.0 17 0.1

5 6 1.5 12 1.0 17 0.1

6 13 1.0 17 0.1

7 15 2.0 17 1.0

8 16 3.0 17 1.0

9

10

11

12

13

14

15

16

17 18 1.0

18 19 1.0 20 0.1 21 0.1 22 0.1 23 0.1 24 0.1 25 1.0 26 1.0

19 27 3.0
20 21 1.5 24 2.0 28 1.0
21 22 1.5 29 1.0
22 23 1.5 30 1.0
23 24 1.5 31 1.0
24 32 1.0
25 33 2.0
26 34 3.0
27
28
29
30
31
32
33
34

C H O O
6-31g(d',p')

W 0
LANL2DZ

W 0
LANL2DZ

Coordinates of [CpW(CO)₃]₂ Used for TD-DFT Calculation

C	0.96788879	1.06864502	-1.58541684
C	2.31778813	-1.90840599	1.15738207
C	1.60497479	-2.33819046	-0.00082494
C	2.31880913	-1.90780341	-1.15819751
C	3.48504084	-1.21583361	-0.71894715
C	3.48444858	-1.21622841	0.71946034
C	2.85928072	1.67565331	0.00022141
C	0.96805612	1.06801307	1.58590852
H	2.02294345	-2.08809703	2.18302178
H	0.68148407	-2.90084307	-0.00153240
H	2.02441333	-2.08659844	-2.18414067
H	4.25359630	-0.79506903	-1.35507228
H	4.25255343	-0.79611373	1.35660029
O	0.65249319	1.62395977	-2.55566960
O	3.58767721	2.57580986	0.00024553
O	0.65249383	1.62292352	2.55635490
W	1.66558475	0.09420967	0.00002236
W	-1.66554072	-0.09416419	-0.00003800
C	-0.96793985	-1.06865483	1.58540393
C	-2.31788549	1.90844219	-1.15739537
C	-1.60514708	2.33825725	0.00084499

C	-2.31897944	1.90778061	1.15818556
C	-3.48513860	1.21572526	0.71887714
C	-3.48449912	1.21615198	-0.71952519
C	-2.85916935	-1.67564570	-0.00028602
C	-0.96798986	-1.06803554	-1.58583311
O	-0.65266524	-1.62405568	2.55564344
H	-2.02301478	2.08817328	-2.18302392
H	-0.68168753	2.90096478	0.00159309
H	-2.02462745	2.08657224	2.18413988
H	-4.25366602	0.79485454	1.35496661
H	-4.25254352	0.79597428	-1.35669634
O	-3.58731625	-2.57600389	0.00005314
O	-0.65267519	-1.62293446	-2.55635811

Crystallographic Details for [CpW(CO)₃(NCCH₃)] [PF₆]

Data collection

An orange crystal (approximate dimensions 0.070 x 0.030 x 0.030 mm³) was placed onto the tip of MiTeGen and mounted on a Bruker D8 VENTURE diffractometer and measured at 150 K. A preliminary set of cell constants was calculated from reflections harvested from a set of 180 frames. These initial sets of frames were oriented such half a sphere in the reciprocal space was surveyed. This produced initial orientation matrices determined from 927 reflections. The data collection was carried out using CuK α radiation (graphite monochromator) with a theta-dependent frame window between 1 to 8 seconds and a detector distance of 3.7 cm. A randomly oriented region of reciprocal space was surveyed to achieve complete data with a redundancy of 5.9. Sections of frames were collected with 1.1° steps in ω and ϕ scans. Data to a resolution of 0.80 Å were considered in the reduction. Final cell constants were calculated from the xyz centroids of 9929 strong reflections from the actual data collection after integration (SAINT).¹ The intensity data were corrected for absorption (SADABS).² Please refer to Table 1 for additional crystal and refinement information.

Structure solution and refinement

The space group $P2_1/n$ was determined based on intensity statistics and systematic absences. The structure was solved using SHELXT³ and refined (full-matrix-least squares) using the Oxford University Crystals for Windows system.⁴ The intrinsic phasing solution provided most non-hydrogen atoms from the E-map. Full-matrix least squares / difference Fourier cycles were performed, which located the remaining non-hydrogen atoms.

Structure 23001 exhibits whole molecule disorder, which was resolved successfully. The two-part disorder was modeled that the occupancies of the major and minor components summed to 1. All non-hydrogen atoms were refined with anisotropic displacement parameters. The hydrogen atoms were placed in ideal positions and refined as riding atoms. The final full matrix least squares refinement converged to $R1 = 0.0416$ and $wR2 = 0.1021$ (F^2 , all data).

Structure description

The structure was found as proposed.

Table S2. Crystal data and structure refinement for 23001.

Empirical formula	C10.00 H8.00 F6 N1.00 O3 P1 W1.00	
Formula weight	518.99	
Crystal color, shape, size	orange block, 0.070 x 0.030 x 0.030 mm ³	
Temperature	150 K	
Wavelength	0.71073 Å	
Crystal system, space group	Monoclinic, P 1 21/n 1	
Unit cell dimensions	a = 11.2330(6) Å	α = 90°.
	b = 7.7115(4) Å	β = 91.7880(10)°.
	c = 16.5205(6) Å	γ = 90°.
Volume	1430.36(12) Å ³	
Z	4	
Density (calculated)	2.410 Mg/m ³	
Absorption coefficient	8.265 mm ⁻¹	
F(000)	968.000	
Data collection		
Diffractometer	Bruker D8 VENTURE, Bruker	
Theta range for data collection	2.161 to 26.406°.	
Index ranges	-13 ≤ h ≤ 13, -9 ≤ k ≤ 9, -19 ≤ l ≤ 19	
Reflections collected	17784	
Independent reflections	2912 [R(int) = 0.000]	
Observed Reflections	2657	
Completeness to theta = 25.878°	99.5 %	
Solution and Refinement		
Absorption correction	Semi-empirical from equivalents	
Max. and min. transmission	0.78 and 0.78	
Solution	Intrinsic phasing methods	
Refinement method	Full-matrix least-squares on F ²	
Weighting scheme	w = [σ ² Fo ² + AP ² + BP] ⁻¹ , with P = (Fo ² + 2 Fc ²)/3, A = 0.025, B = 35.195	
Data / restraints / parameters	2901 / 410 / 399	
Goodness-of-fit on F ²	1.0106	
Final R indices [I > 2σ(I)]	R1 = 0.0416, wR2 = 0.1000	
R indices (all data)	R1 = 0.0454, wR2 = 0.1021	
Largest diff. peak and hole	2.93 and -2.48 e.Å ⁻³	

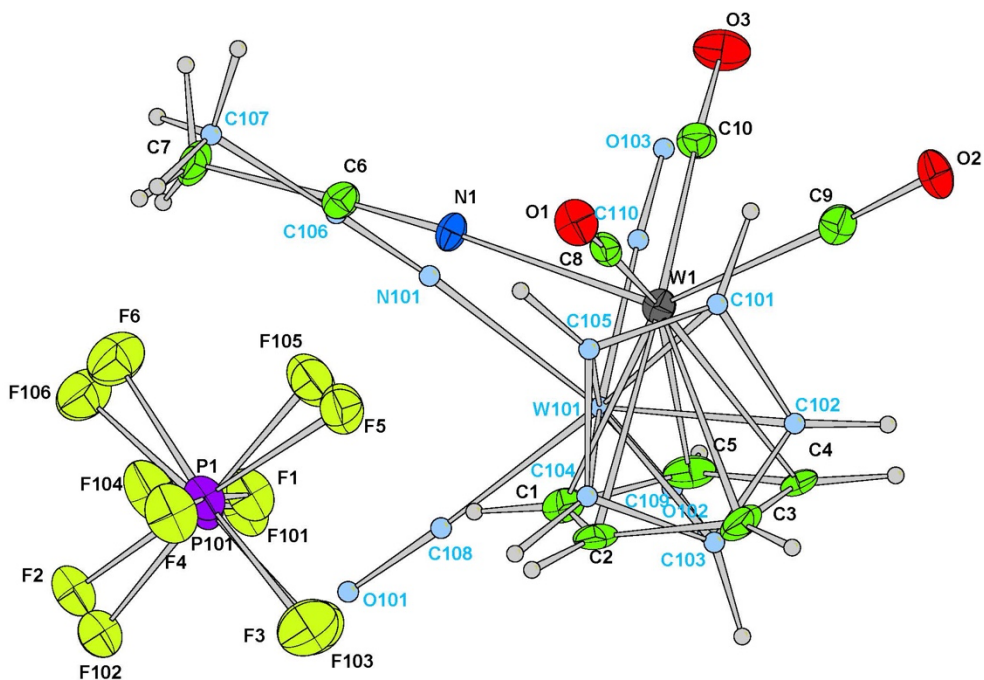


Figure S11. Molecular structure with labels on the asymmetric unit of $[\text{CpW}(\text{CO})_3\text{NCCH}_3][\text{PF}_6]$ with ellipsoids drawn at 50% probability. Gray, blue, red, green, purple, yellow, and white atoms correspond to W, N, O, C, P, F, and H respectively. The minor component of the complex was colored with light blue for clarity.

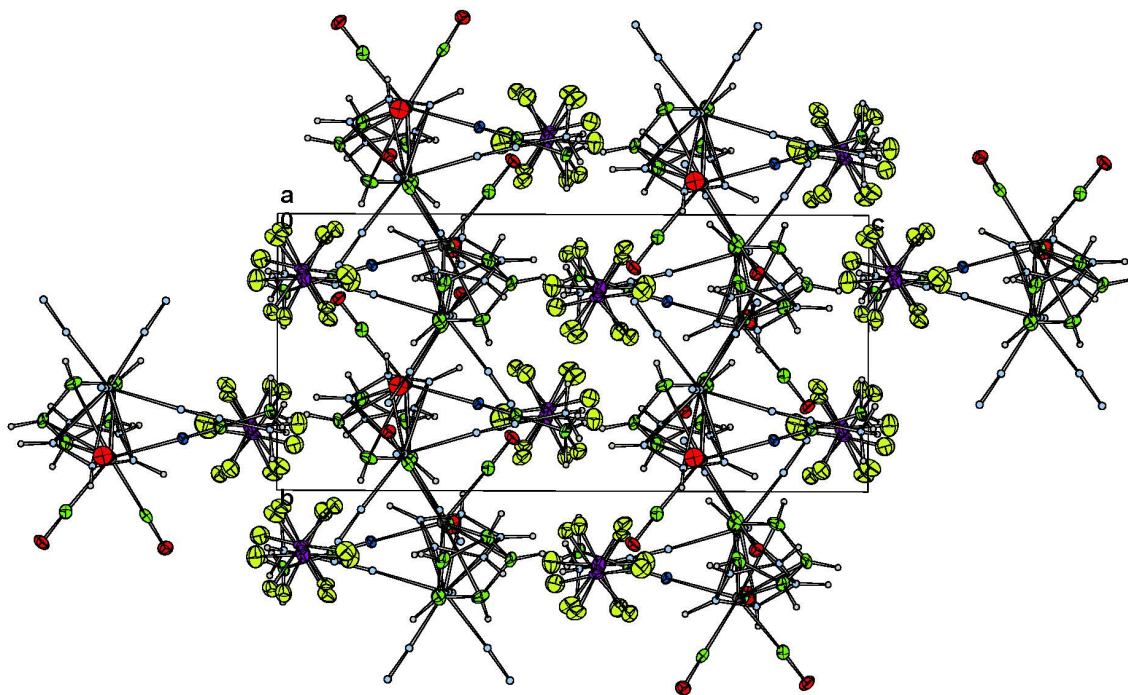


Figure S12. Cell plot, viewed along a- axis.

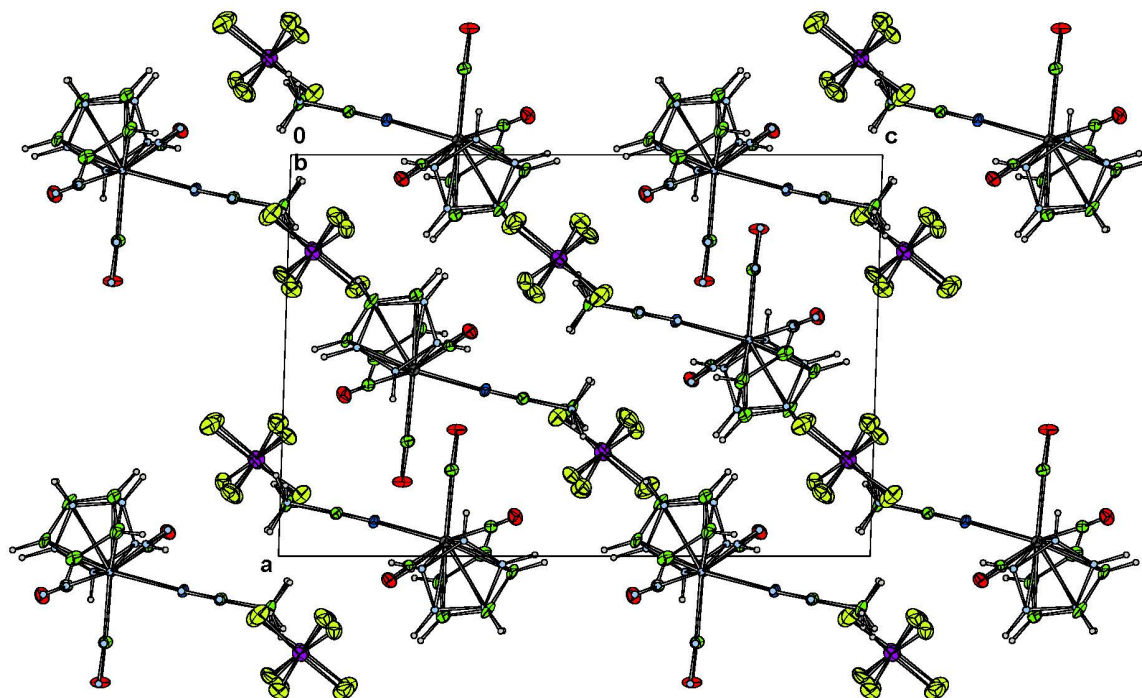


Figure S13. Cell plot, viewed along b- axis.

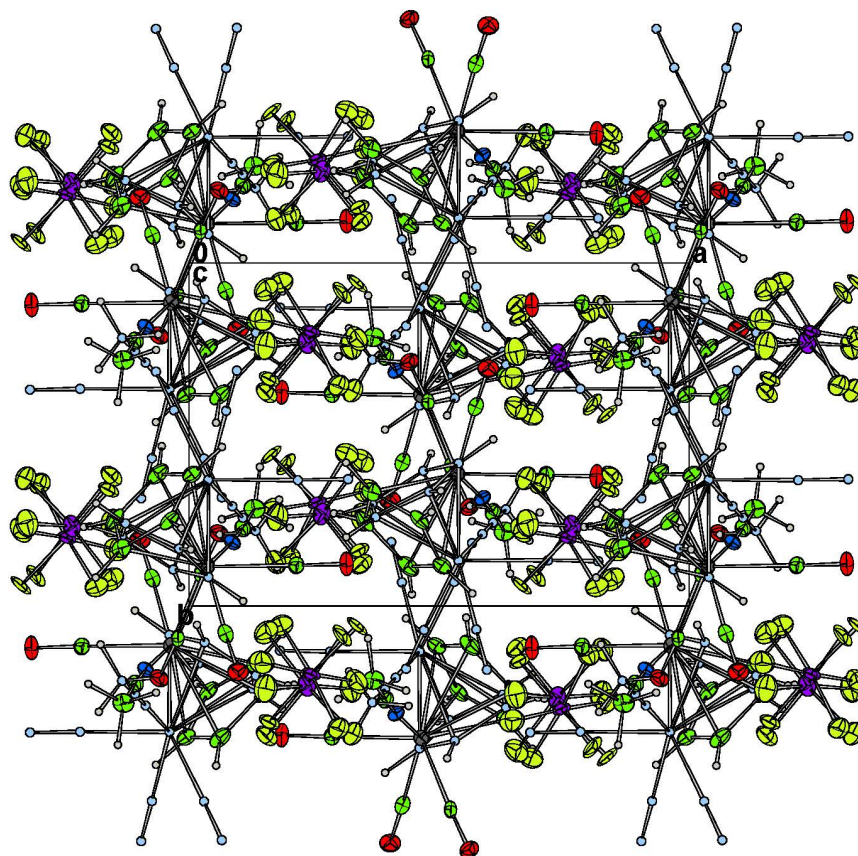


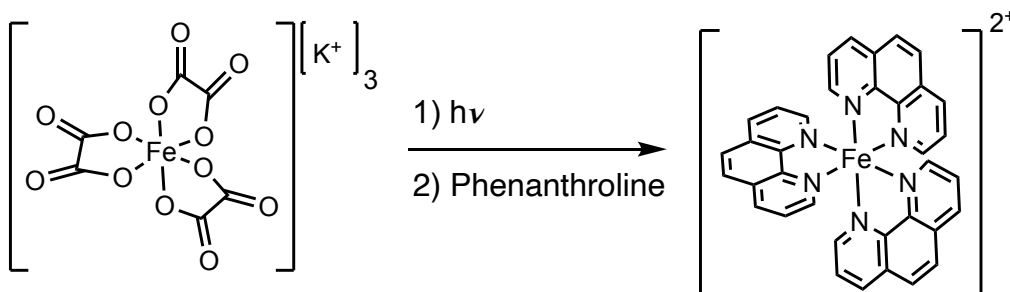
Figure S14. Cell plot, viewed along c- axis.

Actinometry Experiments Using Potassium Ferrioxalate

Preparation of the calibration curve of potassium ferrioxalate was modified from literature procedures.⁵⁻¹⁰ Potassium ferrioxalate was recrystallized in the dark 3 three times. An 84.9 mM solution of potassium ferrioxalate was prepared in 1M H₂SO₄. A 10.2 mM phenanthroline solution, buffered with sodium acetate (5.6144g, 68.44 mmol) was prepared in 0.5 M H₂SO₄. All experiments were conducted with minimal lighting from external sources.

A ThorLabs Multi-wavelength LED lamp (455nm, FWHM = 18 nm) was turned on with a current setting of 25, 50, 100, 150, 200, 250, 300, 400, or 500 mA and left to warm up for 1 hour prior to use. 0.7 mL of the potassium ferrioxalate solution was added to a J. Young tube. Samples were placed 3.5 cm distance away from the lamp and irradiated for 45 (for 500mA), 60 (for 250–400mA), or 120 (for 25-200 mA) seconds. A separate 0.7 mL aliquot of potassium ferrioxalate solution was added to a 10 mL volumetric flask and kept in the dark. After photolysis of the J. Young tube sample, 1 mL of the phenanthroline solution was added to the potassium ferrioxalate solution in both the J. Young tube and in the volumetric flask. Solutions were developed for 10 minutes in the dark to react with the phenanthroline solution. Subsequently, both samples were diluted to 10 mL with reagent grade water using volumetric glassware. A baseline of reagent grade water was taken for UV-vis absorption spectroscopy. A UV-vis absorption spectrum of the control sample kept in the dark was acquired. Then a UV-vis absorption spectrum of the irradiated sample was acquired. There were 3 trials collected for each current setting on the Thor lamp.

Scheme S1. Reaction of potassium ferrioxalate with light and phenanthroline.



The concentration of Fe^{2+} was calculated with the following equation:

$$[Fe^{2+}] = \frac{A_{light} - A_{dark}}{\epsilon_{510\text{ nm}} b}$$

where A_{light} is the absorbance of the irradiated sample, A_{dark} is the absorbance of the sample kept in the dark, $\epsilon_{510\text{ nm}}$ is the extinction coefficient of the Fe phenanthroline complex ($\epsilon = 11,100\text{ M}^{-1}\text{ cm}^{-1}$ at 510 nm), and b is the path length ($b = 1\text{ cm}$) of the cuvette. From there the moles of Fe^{2+} were calculated based on solution volume. Then, the intensity of lamp was calculated using the following equation:

$$I = \frac{\text{Mol } Fe^{2+}}{\phi t a (1 - 10^{-A_\lambda})}$$

where Φ is the quantum yield of potassium ferrioxalate at 455nm ($\Phi = 1.01$)⁶ and A_λ is the absorbance at the 455 nm irradiation wavelength.

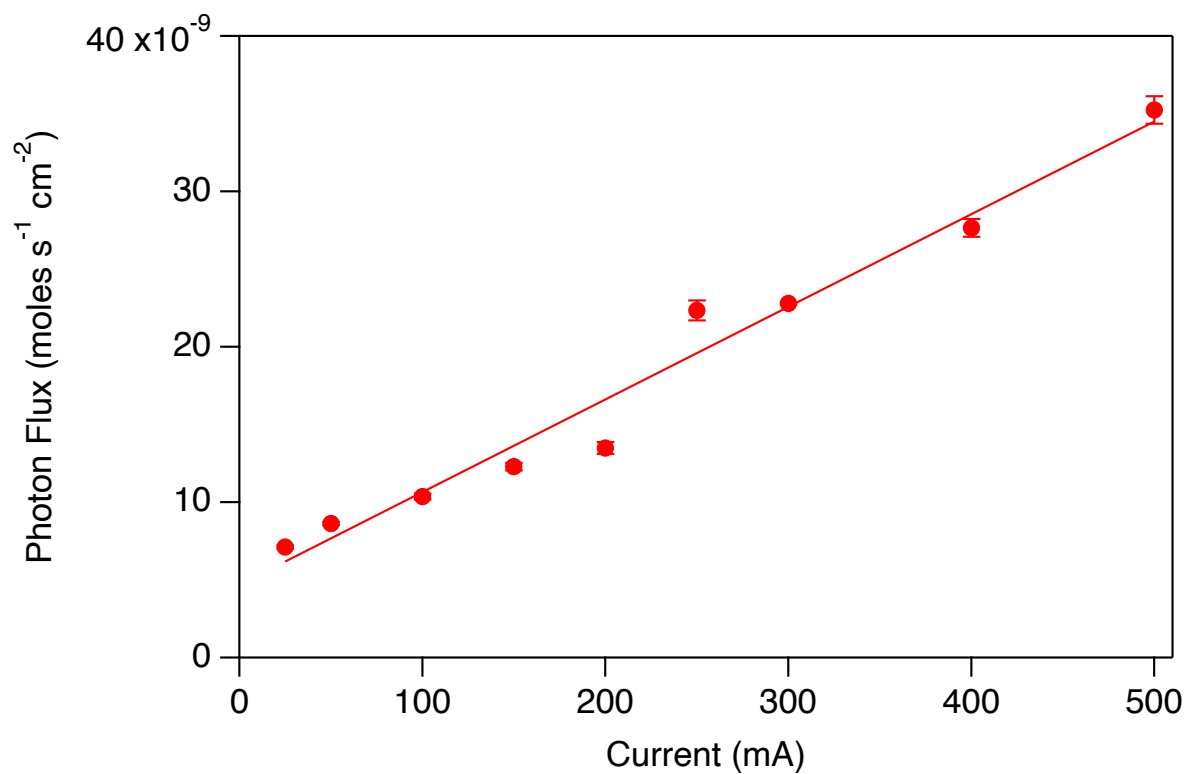


Figure S15. Calibration curve for photon flux to a J. Young tube using potassium ferrioxalate as an actinometer. Current is on the x-axis, representing the intensity setting on the Thor lamp. Error bars are included for the 3 trials. The linear fit for the plot is $y = 5.9603 \times 10^{-11}x + 4.6923 \times 10^{-9}$ with an r^2 value of 0.9702.

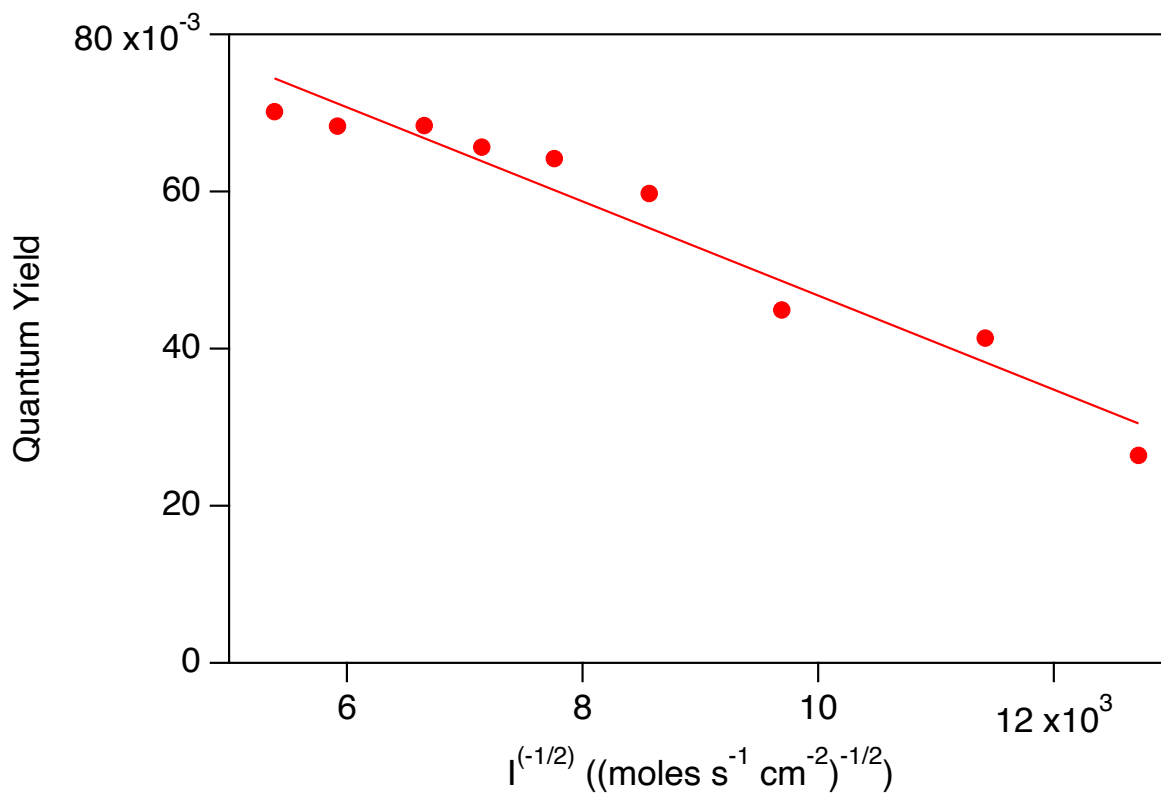
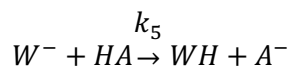
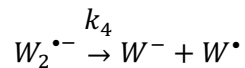
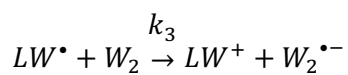
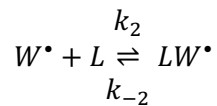
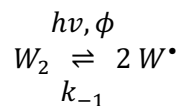


Figure S16. Quantum yield for $\text{CpW}(\text{CO})_3\text{H}$ formation upon irradiation of $[\text{CpW}(\text{CO})_3]_2$ with ca. 67 mM $[\text{PyH}][\text{BF}_4]$ plotted vs. $I^{-1/2}$ (I = photon flux on our sample in $\text{mol photons s}^{-1}$) of the ThorLabs Multi-wavelength LED lamp (455nm). The linear fit for the plot is $y = -5.99 \times 10^{-6} x + 0.1067$, $r^2 = 0.9434$.

Steady-State Approximation

Derivation of Rate Laws for the Radical Chain Mechanism

Scheme S1. Radical chain mechanism



Rate law for consumption of $[CpW(CO)_3]_2$

$$-\frac{d[W_2]}{dt} = I\phi - k_{-1}[W^\bullet]^2 + k_3[W_2][LW^\bullet]$$

Eq. S1

The steady-state approximation for the concentrations of $[\text{CpW}(\text{CO})_3]^*$, $[\text{CpW}(\text{CO})_3\text{L}]^*$, and $[\text{CpW}(\text{CO})_3]_2^{*-}$ can be applied by assuming:

$$\frac{d[W^*]}{dt} = 0 = 2I\phi - 2k_{-1}[W^*]^2 - k_2[W^*][L] + k_{-2}[LW^*] + k_4[W_2^{*-}] \quad \text{Eq. S2}$$

$$\frac{d[LW^*]}{dt} = 0 = k_2[W^*][L] - k_{-2}[LW^*] - k_3[W_2][LW^*] \quad \text{Eq. S3}$$

$$\frac{d[W_2^{*-}]}{dt} = 0 = k_3[W_2][LW^*] - k_4[W_2^{*-}] \quad \text{Eq. S4}$$

From there, the sum of Eqs. S2–S4 yields Eq. S5

$$0 = 2I\phi - 2k_{-1}[W^*]^2 \quad \text{Eq. S5}$$

This expression yields the steady-state concentration of $\text{CpW}(\text{CO})_3^*$

$$[W^*] = \sqrt{\frac{I\phi}{k_{-1}}} \quad \text{Eq. S6}$$

And from Eq. S5 and Eq. S3, we can learn the steady state concentration of $\text{CpW}(\text{CO})_3\text{L}^*$

$$[LW^*] = \frac{k_2\sqrt{\frac{I\phi}{k_{-1}}}[L]}{k_{-2}+k_3[W_2]} \quad \text{Eq. S7}$$

Assuming $k_{-2} \gg k_3[W_2]$, Eq. S7 can be simplified to

$$[LW^*] = \frac{k_2}{k_{-2}}\sqrt{\frac{I\phi}{k_{-1}}}[L] \quad \text{Eq. S8}$$

From there, Eqs. S6 and S8 can be input to Eq. S1, we obtain

$$-\frac{d[W_2]}{dt} = I\phi - \frac{k_{-1}}{k_{-1}}I\phi + \frac{k_3k_2}{k_{-2}}\sqrt{\frac{I\phi}{k_{-1}}}[W_2][L] = \frac{k_3k_2}{k_{-2}\sqrt{k_{-1}}}\sqrt{I\phi}[W_2][L] \quad \text{Eq. S9}$$

Assuming that the rate of $[\text{CpW}(\text{CO})_3]_2$ disappearance is a proxy for $\text{CpW}(\text{CO})_3\text{H}$ formation

$$-\frac{d[W_2]}{dt} = \frac{d[WH]}{dt} \quad \text{Eq. 10}$$

And that $\frac{d[WH]}{dt}$ divided by photon flux on the sample area (I , which as units of mol photons s^{-1})

yields the quantum yield Φ , Eq. S11 tells us that Φ correlates with $\sqrt{\frac{1}{I}}$

$$\Phi = \frac{k_3k_2}{k_{-2}\sqrt{k_{-1}}}\sqrt{\frac{\phi}{I}}[W_2][L] \quad \text{Eq. S11}$$

Reference:

- (1) SAINT, Bruker Analytical X-Ray Systems, Madison, WI.
- (2) An empirical correction for absorption anisotropy, R. Blessing, *Acta Cryst.* A51, 33 - 38 (1995).
- (3) Sheldrick, G. M. (2015): SHELXT – Integrated space-group and crystal-structure determination. *Acta Cryst.* A71, 3-8.
- (4) Betteridge, P. W.; Carruthers, J. R.; Cooper, R. I.; Prout, K.; Watkin, D. J. *J. Appl. Cryst.* **2003**, 36, 1487
- (5) Rabani, J.; Mamane, H.; Pousty, D.; Bolton, J. R. Practical Chemical Actinometry—A Review. *Photochem. Photobiol.* **2021**, 97 (5), 873–902.
- (6) Pitre, S. P.; McTiernan, C. D.; Vine, W.; Dipucchio, R.; Grenier, M.; Scaiano, J. C. Visible-Light Actinometry and Intermittent Illumination as Convenient Tools to Study Ru(Bpy)₃Cl₂ Mediated Photoredox Transformations. *Sci. Reports 2015 51* **2015**, 5 (1), 1–10.
- (7) Bolton, J. R.; Stefan, M. I.; Shaw, P. S.; Lykke, K. R. Determination of the Quantum Yields of the Potassium Ferrioxalate and Potassium Iodide-Iodate Actinometers and a Method for the Calibration of Radiometer Detectors. *J. Photochem. Photobiol. A Chem.* **2011**, 222 (1), 166–169.
- (8) Hatchard, C. G.; Parker, C. A. A New Sensitive Chemical Actinometer - II. Potassium Ferrioxalate as a Standard Chemical Actinometer. *Proc. R. Soc. London. Ser. A. Math. Phys. Sci.* **1956**, 235 (1203), 518–536.
- (9) Schendzielorz, F.; Finger, M.; Abbenseth, J.; Würtele, C.; Krewald, V.; Schneider, S. Metal-Ligand Cooperative Synthesis of Benzonitrile by Electrochemical Reduction and Photolytic Splitting of Dinitrogen. *Angew. Chemie - Int. Ed.* **2019**, 58 (3), 830–834.
- (10) Bruch, Q. J.; Connor, G. P.; Chen, C. H.; Holland, P. L.; Mayer, J. M.; Hasanayn, F.; Miller, A. J. M. Dinitrogen Reduction to Ammonium at Rhenium Utilizing Light and Proton-Coupled Electron Transfer. *J. Am. Chem. Soc.* **2019**, 141 (51), 20198–20208.